11-15-2008

The Parkinson's Disease Protein α-Synuclein Disrupts Cellular Rab Homeostasis

Aaron D. Gitler
Howard Hughes Medical Institute

Brooke J. Bevis
Howard Hughes Medical Institute

James Shorter
Howard Hughes Medical Institute

Katherine E. Strathearn
Purdue University

Shusei Hamamichi
University of Alabama

See next page for additional authors

The Parkinson's disease protein α-synuclein disrupts cellular Rab homeostasis

Aaron D. Gitler*†, Brooke J. Bevis*, James Shorter*‡, Katherine E. Strathearn§, Shusei Hamamichi¶, Linhui Julie Su*, Kim A. Caldwell¶, Guy A. Caldwell¶, Jean-Christophe Rochet§, J. Michael McCaffery‖, Charles Barlowe**, and Susan Lindquist*††

*Whitehead Institute for Biomedical Research and Howard Hughes Medical Institute, Cambridge, MA 02142; §Department of Medicinal Chemistry and Molecular Pharmacology, Purdue University, West Lafayette, IN 47907; ¶Department of Biological Sciences, University of Alabama, Tuscaloosa, AL 35487; ‖Integrated Imaging Center and Department of Biology, Johns Hopkins University, Baltimore, MD 21218; **Department of Biochemistry, Dartmouth Medical School, Hanover, NH 03755; and Departments of †Cell and Developmental Biology and ‡Biochemistry and Biophysics, University of Pennsylvania School of Medicine, Philadelphia, PA 19104

Contributed by Susan Lindquist, November 15, 2007 (sent for review August 20, 2007)

α-Synuclein (α-syn), a protein of unknown function, is the most abundant protein in Lewy bodies, the histological hallmark of Parkinson's disease (PD). In yeast α-syn inhibits endoplasmic reticulum (ER)-to-Golgi (ER→Golgi) vesicle trafficking, which is rescued by overexpression of a Rab GTPase that regulates ER→Golgi trafficking. The homologous Rab1 rescues α-syn toxicity in dopaminergic neuronal models of PD. Here we investigate this conserved feature of α-syn pathobiology. In a cell-free system with purified transport factors α-syn inhibited ER→Golgi trafficking in an α-syn dose-dependent manner. Vesicles budded efficiently from the ER, but their docking or fusion to Golgi membranes was inhibited. Thus, the *in vivo* trafficking problem is due to a direct effect of α-syn on the transport machinery. By ultrastructural analysis the earliest *in vivo* defect was an accumulation of morphologically undocked vesicles, starting near the plasma membrane and growing into massive intracellular vesicular clusters in a dose-dependent manner. By immunofluorescence/immunoelectron microscopy, these clusters were associated both with α-syn and with diverse vesicle markers, suggesting that α-syn can impair multiple trafficking steps. Other Rabs did not ameliorate α-syn toxicity in yeast, but RAB3A, which is highly expressed in neurons and localized to presynaptic termini, and RAB8A, which is localized to post-Golgi vesicles, suppressed toxicity in neuronal models of PD. Thus, α-syn causes general defects in vesicle trafficking, to which dopaminergic neurons are especially sensitive.

endoplasmic reticulum | Rab GTPase | yeasts | vesicle trafficking | Golgi

The protein α-Synuclein (α-syn) is a small presynaptic protein of undefined function implicated in several neurodegenerative disorders, including Parkinson's disease (PD), known collectively as the synucleinopathies (1). Mutations in α-syn or overexpression of the WT gene result in early-onset PD in rare familial forms of the disease. But α-syn is also implicated in the more common sporadic forms. α-Syn has the propensity to aggregate and is found in Lewy bodies, cardinal pathological features of PD (2).

α-Syn was initially identified as a synaptic vesicle-associated protein, although it has also been localized to the cytosol and nucleus (3, 4). α-Syn peripherally associates with synaptic vesicles both *in vitro* and *in vivo* (5, 6). Indeed, association with phospholipid-containing vesicle membranes induces natively unfolded α-syn to adopt an amphipathic α-helical secondary structure (7, 8). In certain contexts, membrane association by α-syn is critical for mediating both its toxic and normal functions (9–11).

Several lines of evidence suggest some role for α-syn trafficking at the synapse. α-Syn knockout mice are grossly normal but exhibit reduced synaptic vesicle reserve pools (12) and enhanced activity-dependent dopamine release (13), both effects likely attributable to precocious vesicle fusion and exocytosis. Conversely, neuronal cells overexpressing α-syn exhibit decreased evoked neurotransmitter release owing to an increase in the pool of docked, but not yet fused, secretory vesicles (14, 15). Other studies with transgenic and knockout mice suggest that α-syn might function as a chaperone for the assembly of SNARE protein complexes that are necessary for vesicle fusion with the plasma membrane (9).

A genetic screen in *Saccharomyces cerevisiae* resulted in the identification of endoplasmic reticulum (ER)→Golgi trafficking genes as potent modifiers of α-syn-induced cellular toxicity (16). Moreover, α-syn caused two different cargoes that undergo different posttranslational modifications en route from the ER to the Golgi to the vacuole, to stall in a pre-Golgi compartment (16). α-Syn expression also resulted in the accumulation of lipid droplets and the production of reactive oxygen species (10), but these occurred after the block in trafficking (ref. 16 and our unpublished data). Thus, transport defects make an important early contribution to pathology.

Here we used *in vitro* transport assays, electron microscopy (EM), and *in vivo* imaging to investigate the nature of α-syn-induced trafficking defects. *In vitro* α-Syn specifically inhibited vesicle docking and/or fusion, and this resulted in the accumulation of transport vesicles *in vivo*. α-Syn strongly colocalized with these vesicles, which were variable in size and staining properties. Indeed, in addition to Ypt1, the Rab that functions in ER→Golgi transport, several other Rabs colocalized with α-syn clusters. Only the ER→Golgi Rab Ypt1 rescued toxicity in yeast, but we reasoned that the distinct biology of dopaminergic neurons might make them more sensitive to perturbations in other trafficking steps. RAB8A is the Rab most closely related to Rab1 by sequence homology, but it functions in post-Golgi trafficking. RAB3A is specific to neurons (17), where it concentrates at presynaptic sites and plays a role in tethering and docking neurotransmitter vesicles in preparation for fusion and release. Both of these Rabs rescued α-syn-induced degeneration in our neuronal models of PD. Our findings provide a molecular explanation for a connection between the normal and pathogenic functions of α-syn. They also indicate that the highly

Author contributions: A.D.G. and B.J.B. contributed equally to this work; A.D.G., B.J.B., J.S., K.E.S., L.J.S., K.A.C., G.A.C., J.-C.R., J.M.M., C.B., and S.L. designed research; A.D.G., B.J.B., K.E.S., S.H., L.J.S., J.M.M., and C.B. performed research; J.S. contributed new reagents/analytic tools; A.D.G., B.J.B., J.S., K.E.S., L.J.S., K.A.C., G.A.C., J.-C.R., J.M.M., C.B., and S.L. analyzed data; and A.D.G., J.S., and S.L. wrote the paper.

Conflict of interest statement: S.L. is a cofounder of and owns stock in FoldRx Pharmaceuticals, a company developing therapies for diseases of protein misfolding, including Parkinson's disease. A.D.G. and S.L. are inventors on patents and patent applications that have been licensed to FoldRx Pharmaceuticals. J.-C.R. receives funds from FoldRx Pharmaceuticals as part of a compound-testing agreement between the company and his laboratory.

††To whom correspondence should be addressed at: Whitehead Institute for Biomedical Research, 9 Cambridge Center, Cambridge, MA 02142. E-mail: lindquist_admin@wi.mit.edu.

This article contains supporting information online at www.pnas.org/cgi/content/full/0710685105/DC1.

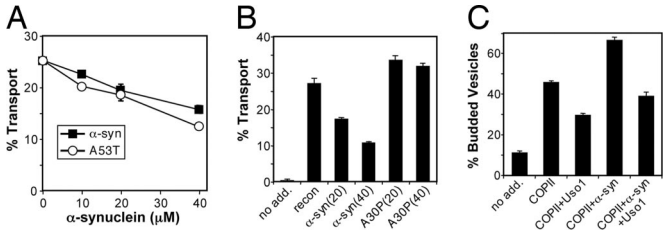

Fig. 1. α-Syn accumulation inhibits *in vitro* ER→Golgi vesicular transport. (*A*) Reconstituted transport reactions in washed semiintact yeast cells containing [^{35}S]glyco-pro-α-factor were incubated with increasing amounts of purified α-syn or the α-syn A53T variant. After 60 min at 25°C, the amount of Golgi-modified [^{35}S]glyco-pro-α-factor was measured to determine transport efficiency. Transport in the absence of reconstitution factors was 2.4%, and plots represent levels minus this background. (*B*) *In vitro* reactions as in *A* comparing the influence of α-syn and the A30P variant on reconstituted transport when added at 20 μM and 40 μM. (*C*) Semiintact cells as in *A* were incubated with COPII proteins or COPII plus Uso1 to measure budding and tethering in the presence or absence of α-syn (40 μM). After 25 min at 25°C, freely diffusible vesicles containing [^{35}S]glyco-pro-α-factor were separated from semiintact cells by centrifugation, and percentages of budded vesicles were determined.

specific pathologies found in the synucleinopathies are not due to biological processes that are restricted to the affected cells. Rather, they are due to the particular vulnerability of neurons (with their generally more extreme trafficking requirements) and dopaminergic neurons (with their relatively problematic neurotransmitter) to a general cellular defect.

Results

α-Syn Inhibits a Specific Step in Transport. ER→Golgi trafficking involves a series of steps, consisting of COPII-dependent vesicle budding from the ER, tethering and docking to target membranes, and finally SNARE protein-dependent vesicle fusion (18). We first asked whether α-syn would inhibit ER→Golgi transport in a reconstituted cell-free assay (19). This assay measures the amount of ER-localized [^{35}S]glyco-pro-α-factor that is transported to the Golgi by detecting a Golgi-specific carbohydrate modification (α-1,6-mannose). WT yeast cells not expressing α-syn were permeabilized and washed to deplete them of soluble proteins. ER membranes in these "semiintact" cells were then loaded with [^{35}S]glyco-pro-α-factor and incubated with or without the purified coat proteins and fusion factors that reconstitute *in vitro* transport (19). The factors resulted in an ≈10-fold increase (from 2.4% to 27.7%) in ER→Golgi transport. Addition of purified soluble α-syn inhibited this transport in a dose-dependent manner (Fig. 1*A*). WT α-syn and a point mutation (A53) that causes early-onset PD in humans and is more toxic than WT α-syn in yeast had the same effect. The increased toxicity of A53T may be downstream of the trafficking defect, perhaps related to its greater tendency to aggregate (20). Importantly, another α-syn point mutant (A30P), which does not bind membranes and is not toxic in yeast (10, 21), did not inhibit transport (Fig. 1*B*), nor did an unrelated control protein, soybean trypsin inhibitor (data not shown). Thus, the strong effects of α-syn on ER→Golgi trafficking observed *in vivo* (16) are likely attributable to its specific interactions with the trafficking machinery rather than to indirect effects on signaling cascades or other perturbations.

Next we tested subreactions in ER→Golgi transport. We incubated washed semiintact cells containing [^{35}S]glyco-pro-α-factor with COPII proteins and an ATP/GTP regeneration system. During the course of the incubation, freely diffusible ER-derived COPII vesicles were released from the ER. Adding a concentration of α-syn (40 μM) that was sufficient to block transport by 50% actually increased the amount of freely diffusible vesicles (from 45% to 65%) (Fig. 1*C*). Thus, α-syn does not inhibit the budding of vesicles from the ER. The increase in free vesicles seemed likely to reflect inhibition in downstream events. Tethering factors facilitate the docking of vesicles onto target membranes. In the absence of α-syn, adding the tethering factor Uso1 (the yeast homolog of p115 in humans) to vesicle budding reactions reduced the amount of freely diffusible vesicles (from 45% to 29%) because they were now tethered to and pelleted with Golgi acceptor membranes (Fig. 1*B*). Uso1 also reduced the amount of diffusible vesicles (from 65% to 38%) in the presence of α-syn, but there were still more diffusible vesicles than with Uso1 alone (29%) (Fig. 1*C*). Together, these data suggest that α-syn inhibits a late stage of ER→Golgi vesicular transport, perhaps reducing the ability of the Uso1 tethering complex to coordinate the events that lead to membrane fusion. Similar effects have been observed in mammalian transport assays (W. Balch, personal communication).

Vesicles accumulate *in vivo* in a time- and dosage-dependent manner. To evaluate the consequences of α-syn overexpression at an ultrastructural level, we performed thin-section EM. Yeast cells expressing one copy of α-syn (1×, which causes no overt reduction in growth) were compared with two other strains. Each carried two copies of α-syn (2×), but these were integrated at different chromosomal locations. These expressed α-syn at different levels with correspondingly different toxicities. As measured by fluorescence-activated cell sorting (data not shown), the intermediate-toxicity strain (IntTox) expressed ≈30–40% less α-syn than the higher-toxicity strain (HiTox) (10, 16). In all of the strains the α-syn genes were under the control of a galactose-regulated promoter, *GAL1*, to prevent expression in normal media.

After transfer to galactose, cells carrying one copy of α-syn accumulated a small number of vesicles relative to cells carrying the vector alone. Strikingly, it was common to see these vesicles associated with the peripheral ER, consistent with α-syn being a negative regulator of vesicle fusion events (15) (Fig. 2 *A–C*). Such vesicles were rarely if ever seen cells expressing the vector alone. After 3 h of galactose induction in the two-copy HiTox strain, small vesicle clusters accumulated primarily at the cellular periphery, proximal to the peripheral ER and plasma membrane (Fig. 2*D*). At 5 h these clusters had grown massive and intruded into the cell interior, taking on a more juxta-vacuolar/nuclear localization (Fig. 2*E*). Similar vesicles were observed in the two-copy IntTox strain, but they accumulated more slowly and were less abundant at equivalent time points [supporting information (SI) Fig. 5]. Thus, as for trafficking defect in the cell-free assays, the ultrastructural defect in vesicle accumulation was dosage-dependent.

Some of the accumulated vesicles were similar in size (50–70 nm) and appearance to vesicles seen in certain *sec* mutants blocked at the ER→Golgi transport step (22). But many were larger, particularly in the HiTox strain (80–100 nm, some even larger), suggestive of Golgi vesiculation or some fusion of clustered vesicles. Vesicle staining densities were also heterogeneous in these cells.

Fluorescence Microscopy to Visualize α-Syn Dynamics. Fluorescence analysis of α-syn-GFP accumulation revealed an initial concentration at the plasma membrane, followed by the formation of many small α-syn foci near the cell periphery. As with vesicles detected by EM, these grew in size over time and eventually coalesced into a few large intracellular clusters (Fig. 2*H*). Moreover, these foci accumulated more rapidly and grew to larger sizes in HiTox than in IntTox cells (SI Fig. 5 *D–G*). Expressing Ypt1 from the strong *GAL1* promoter rescued the growth defect in IntTox cells (16) and strongly reduced α-syn foci (Fig. 2*I*). Expressing Ypt1 from the weaker *GPD* promoter did not rescue toxicity or eliminate α-syn foci. Even the high levels of *GAL1*-expressed Ypt1 did not eliminate foci or toxicity in HiTox cells (data not shown). Thus, the formation of α-syn foci

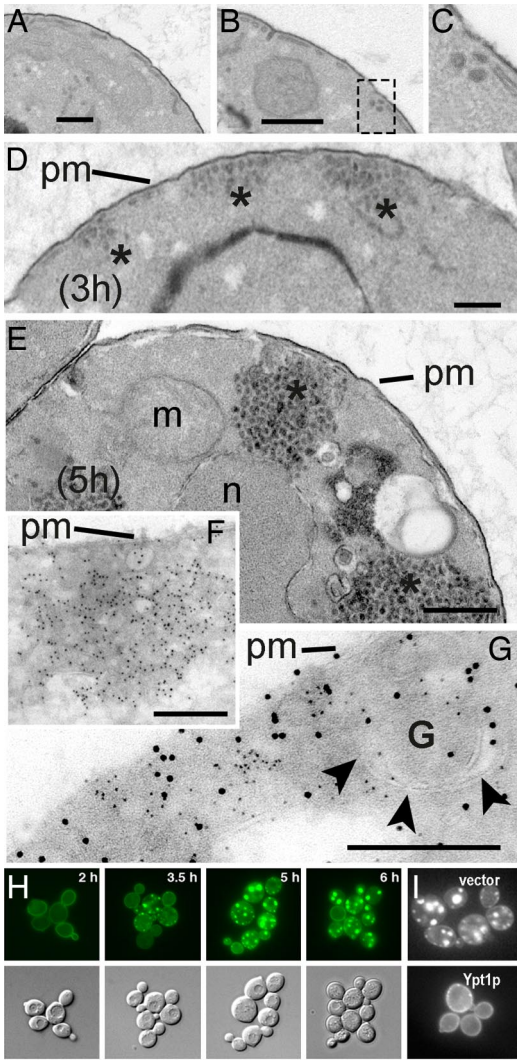

Fig. 2. EM and fluorescence microscopy of α-syn overexpression reveals a time- and dosage-dependent accumulation of transport vesicles. (*A* and *B*) Control strain (*A*) and one-copy (1×) α-syn strain (*B*) at 3 h. (*C*) Higher magnification of vesicles accumulated near peripheral ER at 3 h in the one-copy strain. (*D* and *E*) Time course of α-syn expression [HiTox two-copy (2×) strain] beginning at 3 h (*D*) and proceeding through 5 h (*E*). (*F* and *G*) Indirect immunolabeling of ultrathin cryosections at 5 h after induction demonstrates localization of α-syn-GFP with accumulated vesicle cluster (*F*; 10 nm Au, α-syn-GFP) and colocalization with α-1,6-mannose (*G*; 6 nm Au, α-syn-GFP; 12 nm Au, α-1,6-mannose). m, mitochondria; n, nucleus; pm, plasma membrane; G, Golgi. Asterisks indicate vesicle clusters in *D* and *E*. (*H*) Visualization of α-syn dynamics over time. At early time points (2 h) α-syn-GFP (IntTox 2× strain) localized to the plasma membrane. By 3.5 h many small α-syn-GFP-positive inclusions formed adjacent to the plasma membrane and over time (5 h) began to coalesce into a few large inclusions localized close to the plasma membrane as well as in the interior of the cell (6 h). (*I*) Ypt1 overexpression eliminates α-syn-YFP inclusions. At 6 h, α-syn-YFP-expressing cells contain many vesicular inclusions when transformed with an empty vector. These are eliminated in cells transformed with a Ypt1 expression plasmid. (Scale bars: 0.5 μm.)

depended on both the dosage of α-syn and suppressor and in all cases strongly correlated with toxicity.

Colocalization of α-Syn and Vesicle Clusters. α-Syn interacts with membranes and also has a tendency to misfold and aggregate. The clusters of diverse vesicles might be due to α-syn-coated vesicles providing a multivalent scaffold to trap additional vesicles. If the vesicle defect is a direct result of α-syn's interaction with the trafficking machinery, it should concentrate over accumulating vesicles. To test this, cells expressing an α-syn-GFP fusion were processed for indirect immunoelectron microscopy (immunoEM) with ultrathin cryosections and an antibody directed against GFP.

α-Syn-GFP fusions can behave aberrantly in mammalian cells, but these problems do not occur in yeast. The fusion protein was not cleaved (data not shown), and its biology was identical to untagged α-syn (10). ImmunoEM requires a compromise between mild fixation, needed to preserve antigenic epitopes, and strong fixation, needed to visualize ultrastructure. GFP's resistance to denaturation allowed us to maintain immunoreactivity under conditions where vesicle clusters were still identifiable. α-Syn colocalized with the vesicle clusters very strongly. Thus, as in the cell-free assays, the localization of α-syn to membranes at high concentrations allows vesicles to bud but blocks their docking and/or fusion (Fig. 2*F*).

α-Syn Perturbs Multiple Trafficking Steps. We previously reported that α-syn causes a defect in ER→Golgi trafficking. The diverse size and staining properties of the vesicles detected by EM relative to those expected from a simple ER→Golgi block (23) prompted us to ask whether later stages might also be affected. Indeed, using double-label immunoEM we detected many vesicle clusters containing α-1,6-mannose residues, a Golgi-specific modification (Fig. 2 *F* and *G*; 6 nm Au, α-syn; 12 nm Au, α-1,6-mannose).

ImmunoEM is limited by the availability of high-affinity antibodies against epitopes that are well preserved after fixation. To examine other vesicles we created a panel of centromeric (low-copy) plasmids to express a wide variety of Rabs fused to the cyan fluorescent protein variant Cerulean (24). This enabled the visualization of α-syn-YFP relative to each Rab protein. Similar N-terminal Rab fusions have been shown to be fully functional (25). We took advantage of the fact that *GPD*-driven expression of Ypt1 does not rescue α-syn localization in IntTox cells to examine its localization in comparison with that of other Rabs under the control of the same promoter.

Based on previous reports, except for a slightly increased background staining each Cerulean-Rab fusion protein was localized properly in WT cells (ref. 25 and data not shown) and in cells expressing one copy of α-syn (Fig. 3 *B*, *F*, *J*, *N*, *R*, *V*, and *Z*). However, in cells expressing two copies of α-syn, Rab localization was profoundly altered. Each of the Rabs tested: Ypt1 (ER→Golgi), Ypt31 (late/post-Golgi), Sec4 (secretory vesicles to plasma membrane), Ypt6 (endosome to Golgi), Vps21 and Ypt52 (early endosome to late endosome), and Ypt7 (late endosome to vacuole) colocalized with the α-syn foci (Fig. 3 *D*, *H*, *L*, *P*, *T*, *X*, and *BB*). This colocalization was detectable as soon as strong α-syn foci accumulated.

As a specificity control, we examined localization of the clathrin coat protein Chc1. Clathrin promotes the budding of vesicles from the plasma membrane during endocytosis, but the clathrin cages that engulf these vesicles disassemble immediately after vesicle scission. In striking contrast with the many Rabs we examined, Chc1 localization was not altered in the cells expressing two copies of α-syn, and it did not colocalize with α-syn (Fig. 3 *CC–FF*).

We also looked for colocalization of α-syn with two Golgi proteins: Gos1, a v-SNARE protein that localizes to intra-Golgi vesicles, and Sec7, a GTP exchange factor for Arf that localizes mainly to the late Golgi but not particularly to vesicles. After induction of α-syn, the normally small, Golgi-like puncta formed by Cerulean-Gos1 enlarged and colocalized with the large α-syn foci (Fig. 3 *GG–JJ*). In contrast, Sec7-Cerulean maintained a Golgi-like punctate pattern clearly distinct from the α-syn foci (Fig. 3 *KK–NN*). α-Syn also did not colocalize with Kar1, an ER marker (data not shown). Thus, although α-syn causes a global

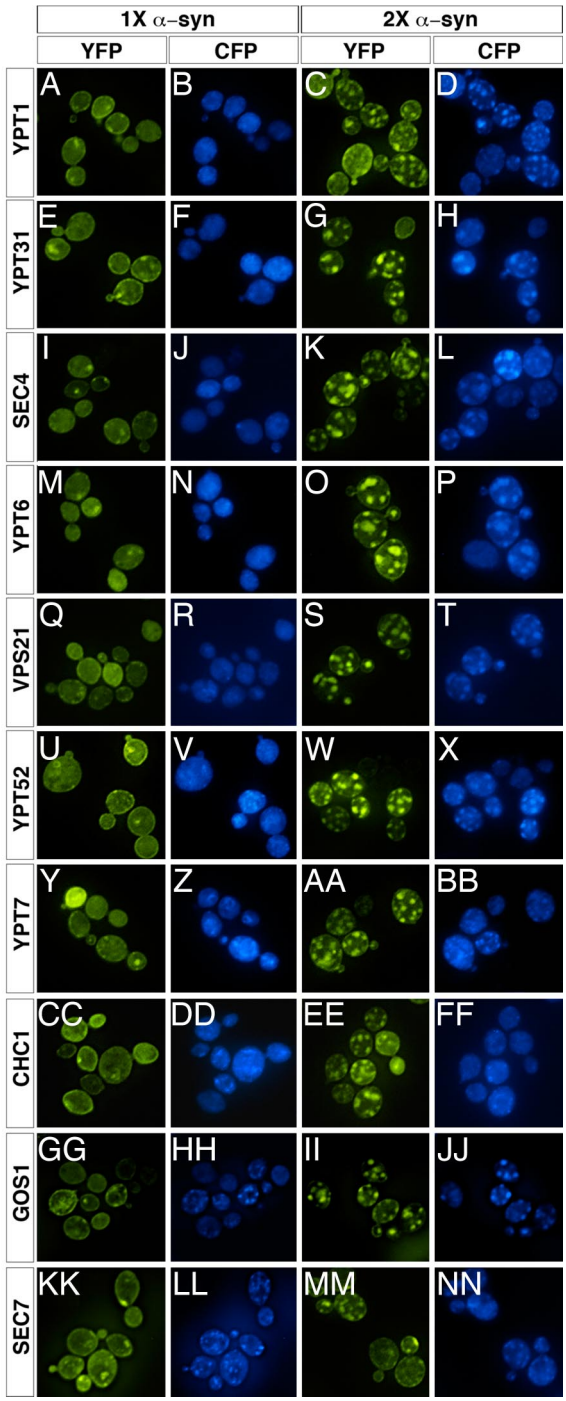

Fig. 3. α-Syn perturbs Rab GTPase homeostasis. Fluorescence microscopy of 1× or 2× α-syn-YFP-expressing cells in the presence of CFP-tagged Rab proteins. In 1× α-syn cells (*A*, *E*, *I*, *M*, *Q*, *U*, *Y*, *CC*, *GG*, and *KK*), each CFP-Rab fusion localized properly based on published reports (*B*, *F*, *J*, *N*, *R*, *V*, and *Z*). In 2× α-syn cells (*C*, *G*, *K*, *O*, *S*, *W*, and *AA*), each Rab was sequestered into the α-syn inclusions (*D*, *H*, *L*, *P*, *T*, *X*, and *BB*). The localization of a CFP fusion to the clathrin heavy chain protein Chc1 (*DD*) was not altered in 2× α-syn cells (*EE* and *FF*), indicating that the presence of a CFP tag was not responsible for the relocalization of the Rab proteins. The Golgi vesicle-localized v-SNARE Gos1 (*HH*) colocalized with α-syn inclusions (*II* and *JJ*), but Sec7p (*KK* and *LL*), an ARF GTP exchange factor, did not (*MM* and *NN*).

defect in trafficking in its pathogenic state it remains highly specific to trafficking vesicles.

These results prompted us to reevaluate previous findings that Ypt1, but not other Rab proteins, suppress α-syn toxicity when overexpressed (16). We overexpressed each of the above Rab proteins from a *GAL1* promoter in IntTox cells. Consistent with our previous report, only Ypt1, and to a very slight degree Ypt6, suppressed toxicity (ref. 16 and data not shown). Apparently Ypt1 is the most critical Rab for suppressing α-syn toxicity in yeast.

RAB3A and RAB8A Protect Against α-Syn-Induced Neuron Loss. The elongated, highly ramified architecture of neuronal cells and the special demands of regulated dopamine release prompted us to ask whether other Rabs might be more important in combating α-syn toxicity in dopaminergic (DA) neurons than they are in yeast. RAB8A, the human homolog of yeast Sec4, is the closest paralog to human RAB1A (55% identical, 75% similar). RAB8A, like yeast Sec4, is localized on post-Golgi vesicles where it facilitates targeting to areas of polarized membrane growth. Given the neuronal specificity of RAB3A expression and the presynaptic terminal localization of α-syn, RAB3A was also an attractive candidate to test.

To evaluate the ability of these Rabs to modify α-syn-induced toxicity in DA neurons we used two very different models. The nematode *Caenorhabditis elegans* offers the advantage of testing DA neurons wired in their natural context to other neurons in a whole animal. Rat primary midbrain cultures lack this advantage but are evolutionarily much closer to human neurons and offer the additional advantage of detecting differential sensitivity of DA neurons (a hallmark of PD) and selective rescue of those neurons that are most affected by α-syn pathology (a therapeutic goal).

In the *C. elegans* PD model a promoter specific to DA neurons ($P_{dat\text{-}1}$) drives expression of WT human α-syn. Because nematode development is so invariable, any deviation from the normal number of DA neurons is highly significant and is readily scored. Six anterior DA neurons are readily visualized in worms carrying a $P_{dat\text{-}1}$::*gfp* construct. For technical ease (16) we previously scored only four. Here we scored all six to provide a more rigorous assay. During the course of aging, overexpression of human α-syn reduced the number of worms with the WT number of neurons to ≈15%. Mouse Rab1 (the clone most readily available and encoding a protein of identical sequence to the human protein) increased it to ≈20%. Human RAB3A increased rescue to 25%, and human RAB8A increased rescue to 40% (Fig. 4*A*). This is the strongest rescue yet achieved with any of the many constructs that have been tested in this nematode model (ref. 16 and our unpublished observations).

The rat primary cell model employs mixed neuronal cultures derived from embryonic rats at day 17. All cell types in the culture were indiscriminately infected with lentivirus encoding a mutant form of α-syn linked to early-onset PD (A53T). DA neurons, scored by tyrosine hydroxylase staining, were more susceptible to the toxicity of this protein relative to total neurons, scored by MAP2 staining (16). Control viruses expressing β-galactosidase had no protective effect (data not shown). In contrast, viruses encoding Rab1, RAB3A, or RAB8A provided strong protection (Fig. 4*B*).

Discussion

Using *in vitro* assays with purified transport components and a combination of *in vivo* assays, we demonstrate that, as α-syn accumulates to toxic levels, transport vesicles bud normally and are targeted to the cell periphery. However, the transition of these vesicles to docking and/or fusion is greatly impaired. Unlike the vesicles accumulating in *sec* mutants blocked at specific trafficking steps, the profusion of vesicles accumulating when α-syn was expressed at toxic levels were heterogeneous in size and staining properties. Furthermore, they were highly clustered, initially forming near the peripheral ER and plasma membrane but later

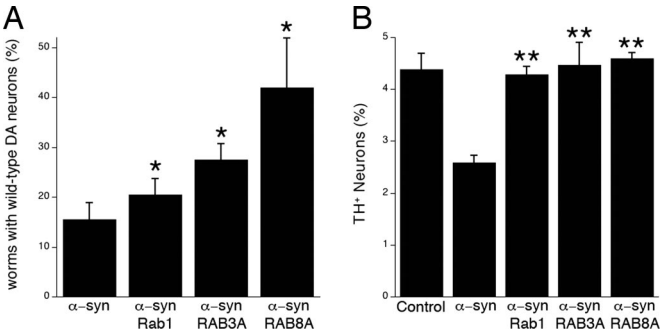

Fig. 4. Rab1, RAB3A, and RAB8A protect against α-syn-induced dopaminergic neuron loss. (*A*) Multiple Rab GTPases ameliorate α-syn-induced neurodegeneration in *C. elegans*. DA neurons of 7-day-old transgenic nematodes overexpressing α-syn along with Rab1, RAB3A, or RAB8A were analyzed. Each Rab tested significantly suppressed α-syn toxicity in worm DA neurons (*, $P < 0.05$, Student's *t* test). For each gene tested, three transgenic lines were analyzed; a worm was scored as WT when all six anterior DA neurons (four CEP and two ADE neurons) were intact. (*B*) Primary rat midbrain cultures were transduced with A53T lentivirus (multiplicity of infection = 5) in the absence or presence of lentivirus encoding RAB3A, RAB8A, or Rab1 (multiplicity of infection of each Rab virus = 2). Control cells were incubated in the absence of lentivirus. Dopaminergic cell viability was determined by staining with antibodies specific for MAP2 and TH and is expressed as the percentage of MAP2-positive neurons that were also TH-positive (two to three independent experiments; at least 100 cells counted per experiment for each treatment). The data are plotted as the mean ± SEM. **, $P < 0.001$ vs. A53T virus alone, one-way ANOVA with Newman–Keuls posttest.

coalescing into intracellular masses. By immunoEM, these vesicles colocalized with α-syn, confirming results of cell-free assays indicating that α-syn effects transport via direct interaction with the trafficking machinery. We speculate that it is three properties of α-syn—its affinity for acidic phospholipid-rich membranes (6), its inhibition of vesicle docking or fusion, and its tendency to misfold and oligomerize (11)—that cause vesicle clustering and contribute to the pathobiology of α-syn.

Although only the ER→Golgi Ypt1 significantly affected α-syn toxicity (ref. 16 and data herein), by EM and fluorescence immunomicroscopy vesicles from different parts of the exocytic and endocytic pathways are sequestered in α-syn clusters. Because several of their associated Rabs are not essential in yeast they might not have been picked up in our genetic screen because perturbations in their function were simply not pivotal to survival. This seems unlikely. Sec4p, like Ypt1, is essential and functions at the last steps of exocytosis, steps analogous to synaptic vesicle docking and fusion in neurons. It might be that Sec4p overexpression does not rescue in yeast simply because its dysfunction in our cells is of secondary importance to that of Ypt1 or because the particular level of expression achieved with our construct was insufficient.

Critically, in higher organisms two other Rab proteins, one chosen because it is a close paralog to Rab1 (RAB8A, the mammalian homolog of Sec4p), the other because it is neuron-specific and functions at the synapse (RAB3A), were able to provide substantial rescue against α-syn-induced degeneration of DA neurons. The fact that rescue was achieved in two very different neuronal models—in the intact nervous system of the nematode and in dispersed primary rat neuronal cultures, which allow assessment of the differential sensitivity and rescue of DA neurons—argues that α-syn broadly perturbs vesicle trafficking and that these perturbations are relevant to its pathobiology. The secretory pathway is highly conserved between yeast and mammals; however, there is higher complexity in the mammalian membrane transport apparatus, as evidenced by the much greater number of Rabs. Evidence for α-syn-mediated disruption of ER→Golgi trafficking has been reported in mammalian cells (ref. 26 and W. Balch, personal communication). And Rab1, which controls this trafficking step, rescues in all three of the systems we employ here. It might be, therefore, that the trafficking defect starts at the ER→Golgi step and that the trapping of other vesicles is secondary to that. Alternatively, α-syn might most strongly affect the very closely related Rab1 and RAB8A, secondarily involving others. Or multiple Rabs might be affected at the same time. In any case, these observations suggest that at least some forms of PD, which would at first sight have appeared to be due to biology highly specific to certain neurons, might actually be caused by defects in very basic aspects of cell biology that particular neurons are simply more sensitive to. Indeed, vesicle accumulations, strikingly similar to what we see in yeast cells, have been observed in neurons before Lewy body formation (27). Furthermore, vesicle accumulations are often found in proximity to Lewy bodies in later stages of disease (28, 29).

Neurons have extremely elongated and highly ramified cellular architectures. Any general trafficking problems would be expected to affect them more strongly than most cells. Furthermore, DA neurons transport a particularly dangerous neurotransmitter. Dopamine is made in the cytoplasm and is highly prone to producing reactive oxygen species until sequestered into vesicles (30–32). A defect in the production of vesicles would lead to a defect in dopamine sequestration, potentially causing some of the oxidative damage that is characteristic of PD. If a defect also exists in later stages of vesicle trafficking, this would catch DA neurons in a triple-sided vise. In addition to increased cytosolic dopamine, there would be fewer dopamine-containing vesicles to release in response to appropriate signals, and the release of those vesicles that are available would be compromised. Why some dopamine neurons are spared and why certain other neurons are susceptible (e.g., pyramidal neuronal loss in the presupplementary motor area) might relate to aspects of biology not captured by α-syn toxicity alone or to other metabolic features (e.g., relative rates of respiration, iron accumulation) that play into α-syn toxicity in a yet undefined way. Indeed, genome-wide genetic analysis in yeast (A.D.G., A. D. Cashikar, K.E.S., S.H., E. Yeger-Lotem, M. Geddie, K. J. Hill, E. Fraenkel, K.A.C., G.A.C., A. A. Cooper, J.-C.R., and S.L., unpublished data) and the effects of chemical compounds on α-syn toxicity in yeast and neurons (L.J.S., T. F. Outeiro, E. Yeger-Lotem, P. K. Auluck, K.E.S., S. Cao, S.H., K. Hill, K.A.C., G. Bell, A. A. Cooper, G.A.C., J.M.M., J.-C.R., and S.L., unpublished data) point to many other features of cell biology that impinge on α-syn toxicity.

A proposed role for α-syn under normal physiological conditions, as a negative regulator of synaptic vesicle priming before fusion (14), is completely consistent with our results. Such a function might be hyperactivated during pathogenesis because of inappropriate α-syn expression or defective α-syn degradation, both with the potential to exacerbate problems with α-syn oligomerization and vesicle trapping. Thus, the normal and toxic functions of α-syn might be more closely related than previously realized (15).

Materials and Methods

Yeast Strains and Constructs. Strains were constructed as detailed in *SI Materials and Methods*. In the HiTox strain, two copies of α-syn were integrated into the *URA3* and *TRP1* loci; for the IntTox strain, the α-syn cassettes were integrated at *HIS3* and *TRP1*. For the fluorescence microscopy experiments, fusion constructs were generated by using the pRS series-based Gateway vectors (24). The secretory pathway proteins were cloned into pAG416GPD-Cerulean-ccdB to generate N-terminal fusions to Cerulean, expressed from the GPD promoter. We fused Cerulean to the C terminus of Sec7 using pAG416GPD-ccdB-Cerulean.

***In Vitro* Transport Assays.** α-Syn proteins were purified as described in *SI Materials and Methods*, and protein concentration was determined by Bradford assay in relation to BSA standards. Yeast semiintact cells were prepared from strain CBY740 (*MATα his3 leu2 lys2 ura3*) as described previously (19). *In vitro* assays for vesicle budding, tethering, and fusion have been published previously (19). Plotted data points are the average of duplicate determinations with error bars indicating the range.

Microscopy. Conventional and immunoEM were performed as detailed in *SI Materials and Methods*. For fluorescence microscopy experiments, yeast strains were grown to stationary phase in glucose media. Raffinose media was inoculated with an aliquot of the culture and grown to early- to mid-log phase at 30°C. Cultures were spun down, resuspended in galactose-containing media, and incubated for 6 h to induce expression of α-syn-YFP before being fixed in 4% formaldehyde/50 mM KPi (pH 6.5)/1 mM $MgCl_2$ on ice for 1 h, washed twice in PBS, and resuspended in a small volume of PBS for microscopy studies. Images were obtained by using a Zeiss Axiovert 200 microscope. Z-stacks of several fields were collected, and the images were deblurred by using a nearest neighbor algorithm in Axiovision software.

C. elegans and rat primary midbrain neurons were prepared and maintained following standard procedures and analyzed as described previously (16) with minor modifications detailed in *SI Materials and Methods*.

ACKNOWLEDGMENTS. We thank Blake Roberts and Huan Wang for comments on the manuscript, Christopher Reed and Michelle Husain for excellent EM technical assistance, and Karen Allendoerfer for invaluable help in preparing the manuscript. A.D.G. was a Lilly Fellow of the Life Sciences Research Foundation. J.S. is supported by an American Heart Association Scientist Development Grant. L.J.S. was supported by an American Cancer Society fellowship. This work was supported by Udall Center Grant NS38372 (to S.L.), National Institutes of Health Grants GM52549 (to C.B.) and NS049221 (to J.-C.R.), and grants from the Whitehead Institute for Biomedical Research Regenerative Biology Initiative (to S.L.), the American Parkinson's Disease Association (to J.-C.R. and G.A.C.), the National Institute of Environmental Health Sciences (to G.A.C.), and the Michael J. Fox Foundation (to G.A.C.).

1. Lee VM, Trojanowski JQ (2006) Mechanisms of Parkinson's disease linked to pathological alpha-synuclein: New targets for drug discovery. *Neuron* 52:33–38.
2. Spillantini MG, *et al.* (1997) Alpha-synuclein in Lewy bodies. *Nature* 388:839–840.
3. Kontopoulos E, Parvin JD, Feany MB (2006) Alpha-synuclein acts in the nucleus to inhibit histone acetylation and promote neurotoxicity. *Hum Mol Genet* 15:3012–3023.
4. Lee HJ, Patel S, Lee SJ (2005) Intravesicular localization and exocytosis of alpha-synuclein and its aggregates. *J Neurosci* 25:6016–6024.
5. Fortin DL, *et al.* (2004) Lipid rafts mediate the synaptic localization of alpha-synuclein. *J Neurosci* 24:6715–6723.
6. Kubo S, *et al.* (2005) A combinatorial code for the interaction of alpha-synuclein with membranes. *J Biol Chem* 280:31664–31672.
7. Eliezer D, Kutluay E, Bussell R, Jr, Browne G (2001) Conformational properties of alpha-synuclein in its free and lipid-associated states. *J Mol Biol* 307:1061–1073.
8. Weinreb PH, Zhen W, Poon AW, Conway KA, Lansbury PT, Jr (1996) NACP, a protein implicated in Alzheimer's disease and learning, is natively unfolded. *Biochemistry* 35:13709–13715.
9. Chandra S, Gallardo G, Fernandez-Chacon R, Schluter OM, Sudhof TC (2005) Alpha-synuclein cooperates with CSPalpha in preventing neurodegeneration. *Cell* 123:383–396.
10. Outeiro TF, Lindquist S (2003) Yeast cells provide insight into alpha-synuclein biology and pathobiology. *Science* 302:1772–1775.
11. Volles MJ, Lansbury PT, Jr (2007) Relationships between the sequence of alpha-synuclein and its membrane affinity, fibrillization propensity, and yeast toxicity. *J Mol Biol* 366:1510–1522.
12. Cabin DE, *et al.* (2002) Synaptic vesicle depletion correlates with attenuated synaptic responses to prolonged repetitive stimulation in mice lacking alpha-synuclein. *J Neurosci* 22:8797–8807.
13. Abeliovich A, *et al.* (2000) Mice lacking alpha-synuclein display functional deficits in the nigrostriatal dopamine system. *Neuron* 25:239–252.
14. Larsen KE, *et al.* (2006) Alpha-synuclein overexpression in PC12 and chromaffin cells impairs catecholamine release by interfering with a late step in exocytosis. *J Neurosci* 26:11915–11922.
15. Gitler AD, Shorter J (2007) Prime time for alpha-synuclein. *J Neurosci* 27:2433–2434.
16. Cooper AA, *et al.* (2006) Alpha-synuclein blocks ER-Golgi traffic and Rab1 rescues neuron loss in Parkinson's models. *Science* 313:324–328.
17. Gurkan C, *et al.* (2005) Large-scale profiling of Rab GTPase trafficking networks: The membrome. *Mol Biol Cell* 16:3847–3864.
18. Pfeffer SR (1999) Transport-vesicle targeting: Tethers before SNAREs. *Nat Cell Biol* 1:E17–E22.
19. Barlowe C (1997) Coupled ER to Golgi transport reconstituted with purified cytosolic proteins. *J Cell Biol* 139:1097–1108.
20. Conway KA, Harper JD, Lansbury PT (1998) Accelerated in vitro fibril formation by a mutant alpha-synuclein linked to early-onset Parkinson disease. *Nat Med* 4:1318–1320.
21. Jo E, Fuller N, Rand RP, St George-Hyslop P, Fraser PE (2002) Defective membrane interactions of familial Parkinson's disease mutant A30P alpha-synuclein. *J Mol Biol* 315:799–807.
22. Novick P, Field C, Schekman R (1980) Identification of 23 complementation groups required for post-translational events in the yeast secretory pathway. *Cell* 21:205–215.
23. Kaiser CA, Schekman R (1990) Distinct sets of SEC genes govern transport vesicle formation and fusion early in the secretory pathway. *Cell* 61:723–733.
24. Alberti S, Gitler AD, Lindquist S (2007) A suite of Gateway cloning vectors for high-throughput genetic analysis in Saccharomyces cerevisiae. *Yeast* 24:913–919.
25. Calero M, *et al.* (2003) Dual prenylation is required for Rab protein localization and function. *Mol Biol Cell* 14:1852–1867.
26. Gosavi N, Lee HJ, Lee JS, Patel S, Lee SJ (2002) Golgi fragmentation occurs in the cells with prefibrillar alpha-synuclein aggregates and precedes the formation of fibrillar inclusion. *J Biol Chem* 277:48984–48992.
27. Hayashida K, Oyanagi S, Mizutani Y, Yokochi M (1993) An early cytoplasmic change before Lewy body maturation: An ultrastructural study of the substantia nigra from an autopsy case of juvenile parkinsonism. *Acta Neuropathol (Berlin)* 85:445–448.
28. Forno LS, Norville RL (1976) Ultrastructure of Lewy bodies in the stellate ganglion. *Acta Neuropathol (Berlin)* 34:183–197.
29. Watanabe I, Vachal E, Tomita T (1977) Dense core vesicles around the Lewy body in incidental Parkinson's disease: An electron microscopic study. *Acta Neuropathol (Berlin)* 39:173–175.
30. Caudle WM, *et al.* (2007) Reduced vesicular storage of dopamine causes progressive nigrostriatal neurodegeneration. *J Neurosci* 27:8138–8148.
31. Lotharius J, Brundin P (2002) Pathogenesis of Parkinson's disease: Dopamine, vesicles and alpha-synuclein. *Nat Rev Neurosci* 3:932–942.
32. Xu J, *et al.* (2002) Dopamine-dependent neurotoxicity of alpha-synuclein: A mechanism for selective neurodegeneration in Parkinson disease. *Nat Med* 8:600–606.